Porous Materials

DOI: 10.1002/anie.200803640

Hierarchically Micro- and Mesoporous Metal–Organic Frameworks with Tunable Porosity**

Ling-Guang Qiu, Tao Xu, Zong-Qun Li, Wei Wang, Yun Wu, Xia Jiang, Xing-You Tian, and Li-De Zhang*

Porous metal–organic frameworks (MOFs) are crystalline materials with pores and channels self-assembled by the bonding of metal ions with multifunctional organic ligands.[1–3] They have attracted attention recently, owing to interest in the creation of nanosized spaces and their potential applications in gas storage,[4] in adsorption and separation,[5] in heterogeneous catalysis,[6] in molecular sensing,[7] and as magnetic materials.[8] Porous MOFs are synthesized under mild conditions, compared with traditional porous carbons and inorganic zeolites, and hold great promise because of their processability, flexibility, structural diversity, and geometrical control. However, to date, porous MOFs are still largely restricted to the microporous regime, despite the negative impact of small pore size on diffusion and mass transfer. Although organic ligands can be designed to create large voids, only sporadic successful examples of the rational design of mesoporous MOFs are found in the literature.[9–13] The inherent reason for this limitation is attributed to the fact that MOFs with large pore sizes are frequently plagued by framework breakdown upon removal of the guest molecules. Another danger is that, even if one is successful in creating a desired framework, the framework itself may occupy intraframework space through interpenetration, leading to a close-packed structure.[1–3] As a result, the development of reliable and reproducible methods to achieve robust mesoporous MOFs with tailored structures and tunable properties remains a great challenge.

Recently, hierarchically porous materials with controlled porosity have also received considerable attention, because they provide many novel properties and have important prospects in practical industrial processes, such as catalysis, adsorption, and chemical sensing.[14] In general, hierarchical pore systems are advantageous, because they feature high pore volumes and large surface areas, together with potentially larger pore sizes. Such structures commonly show improved diffusion of guest molecules through the framework, as larger pores allow for improved molecular accessibility, whereas smaller pores provide high surface areas and large pore volumes.

Herein, we explore a simple and versatile strategy that has allowed us to rationally design and synthesize hierarchically micro- and mesoporous MOFs with adjustable porosity, for the first time. A novel supramolecular template strategy has been successfully applied to design mesostructured MOFs with tunable pore size, pore volume, and surface area (Scheme 1). Although supramolecular aggregates of surfactant molecules, such as micelles, have been widely used to develop various mesoporous molecular sieves and mesostructured metal oxides,[14,15] the application of such supramolecular templates to the design of mesostructured MOFs remains unexplored. Actually, low-molecular-weight organic guests or solvent molecules have been widely chosen as templating agents to avoid framework interpenetration in the synthesis of porous MOFs.[1–3] In many cases, however, template molecules occupy part of the channels in the framework, and the removal of template molecules from the channels usually leads to the collapse of the framework.

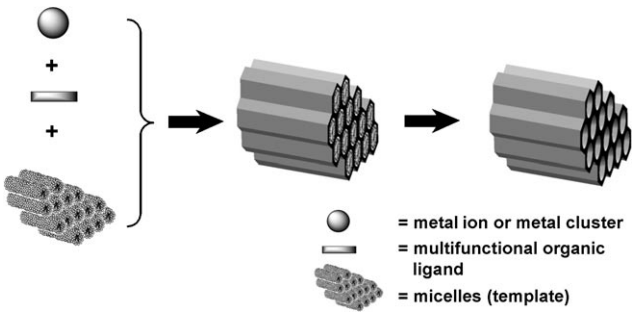

Scheme 1. Mesostructured MOFs self-assembled from metal ions and multifunctional organic ligands in the presence of surfactant micelles as supramolecular templates.

In this work, we used the surfactant cetyltrimethylammonium bromide (CTAB) as a structure-directing agent, and chose Cu^{2+} and benzene-1,3,5-tricarboxylate (btc^{3-}) ions as framework-building blocks to illustrate the supramolecular template strategy for designing and preparing mesostructured MOFs with tailored porosity. A series of hierarchically porous MOFs with adjustable interconnecting micropores and mesopores was prepared by self-assembly of the framework-

[*] Prof. Dr. L.-G. Qiu, T. Xu, Z.-Q. Li, W. Wang, Y. Wu, X. Jiang
School of Chemistry and Chemical Engineering
Anhui University
Hefei 230039 (P.R. China)
Fax: (+86) 551-5107342
E-mail: lgqiu@ahu.edu.cn
Prof. Dr. X.-Y. Tian, Prof. L.-D. Zhang
Institute of Solid State Physics
Chinese Academy of Sciences
Hefei 230031 (P.R. China)

[**] This work was supported by the National Natural Science Foundation of China (20501001), the Key Research Project of Natural Science of the Provincial Bureau of Education, Anhui, China (kj2007A078), and the Selected Financial Support Research Project of the Provincial Bureau of Education, Anhui, China.

Supporting information for this article is available on the WWW under http://dx.doi.org/10.1002/anie.200803640.

building blocks in the presence of surfactant micelles. These mesostructured MOFs possess a mesopore system with diameters tunable from 3.8 to 31.0 nm, depending on the synthetic conditions. Particularly, the mesopore walls in these solids are formed from a crystalline microporous framework containing a 3D system of channels with a pore diameter of 0.82 nm, resulting in hierarchically micro- and mesoporous MOFs (Scheme 2). To our knowledge, this work is the first example of the rational design of hierarchically porous MOFs with tunable porosity.

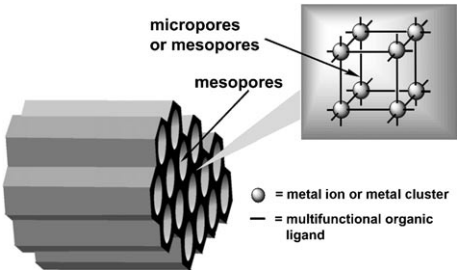

Scheme 2. Mesostructured MOFs in which mesopore walls are constructed from micro- or mesoporous MOFs assembled from metal ions and multifunctional organic ligands.

The solvothermal reaction of cupric nitrate trihydrate and H_3btc in a solution of 50% ethanol by volume in water at 120°C for 12 h resulted in a microporous MOF, $[Cu_3(btc)_2(H_2O)_3]$ (HKUST-1), containing a 3D channel system with a pore diameter of 0.85 nm.[16] As expected, mesostructured MOFs of the same formula were obtained by the reaction of Cu^{2+} ions and H_3btc in the presence of CTAB micelles under similar reaction conditions. Figure 1 shows representative N_2 adsorption–desorption isotherms and distributions of pore

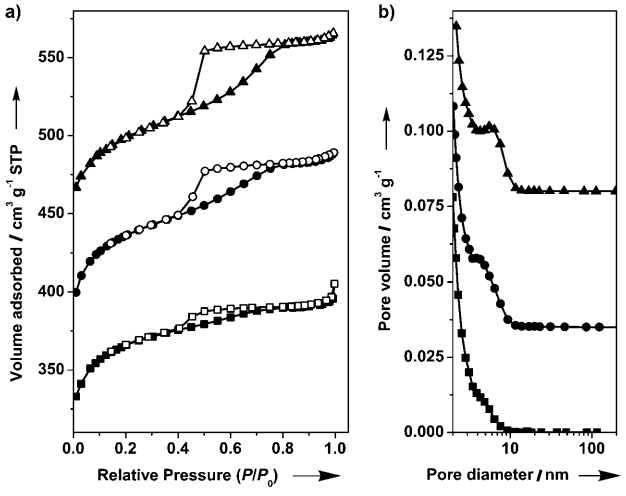

Figure 1. Pore-structure analysis of the hierarchically micro- and mesoporous MOFs **1A** (□), **1B** (○), and **1C** (△). a) N_2 adsorption–desorption isotherms; the isotherms for **1B** and **1C** are vertically offset by 100 and 200 $cm^3 g^{-1}$, respectively. b) Distributions of pore diameters obtained using the Barrett–Joyner–Halenda (BJH) method; the distributions for **1B** and **1C** are vertically offset by 0.035 and 0.08 $cm^3 g^{-1}$, respectively.

diameters for the mesostructured $[Cu_3(btc)_2(H_2O)_3]$ MOFs synthesized at CTAB/Cu^{2+} molar ratios of 0.15 (**1A**), 0.30 (**1B**), and 0.60 (**1C**). All three samples exhibit N_2 adsorption–desorption isotherms of a mode intermediate between type I, which is related to microporous materials, and type IV, which is related to mesoporous materials. The presence of a pronounced hysteresis loop in the N_2 isotherms is indicative of a porous structure with a 3D intersection network.[17] Furthermore, high N_2 adsorption capacities (330 $cm^3 g^{-1}$ for **1A**, 300 $cm^3 g^{-1}$ for **1B**, and 267 $cm^3 g^{-1}$ for **1C**) are observed for these mesostructured MOFs, even when the relative pressure (P/P_0) is as low as 0.01 (Figure 1a), suggesting that the as-synthesized MOFs are mesoporous with a microporous contribution. This result is confirmed by an analysis of the distribution of pore diameters for **1C**. In addition to mesopores with a diameter of 5.6 nm, the solid contains micropores with a diameter of 0.82 nm (see Figure S1 in the Supporting Information), which is consistent with the micropore diameter (0.85 nm) estimated from crystallographic data for microporous $[Cu_3(btc)_2(H_2O)_3]$.[16] All these results reveal that the reaction of Cu^{2+} ions and H_3btc in the presence of a structure-directing agent (CTAB micelles) results in mesostructured MOFs in which the mesopore walls are constructed from the microporous framework $[Cu_3(btc)_2(H_2O)_3]$.

The porosity properties of the mesostructured MOFs are tunable by varying the CTAB/Cu^{2+} molar ratio. As can be seen from Figure 1b and Table 1, the mesopore diameter of these mesostructured MOFs increases from 3.8 to 5.6 nm with increasing CTAB/Cu^{2+} molar ratio from 0.15 to 0.60. Accordingly, the Brunauer–Emmett–Teller (BET) specific surface area (S_{BET}) measured from the N_2 isotherms decreases from 1225 to 905 $m^2 g^{-1}$ (Table 1). In addition, the mesopore-to-micropore surface-area ratio (S_{meso}/S_{micro}) and the mesopore-to-micropore pore-volume ratio (V_{meso}/V_{micro}) can also be tuned by varying the CTAB/Cu^{2+} molar ratio. The S_{meso}/S_{micro} ratio and the V_{meso}/V_{micro} ratio increase gradually from 0.24 to 0.34 and from 0.24 to 0.44, respectively, with an increase in the CTAB/Cu^{2+} molar ratio from 0.15 to 0.60 (Table 1).

Although it has been clearly demonstrated that hierarchically micro- and mesoporous MOFs with tunable porosity can be obtained using a supramolecular template strategy, the mesopore diameters of the MOFs synthesized using CTAB as a structure-directing agent are still limited to 5.6 nm. To obtain mesostructured MOFs with much larger mesopore sizes, a hydrophobic organic compound, 1,3,5-trimethylbenzene (TMB), was chosen as an auxiliary structure-directing agent to swell the CTAB micelles. The original work of the Mobil group on the assembly of MCM-41 silicas showed that mesopore size could be tuned by incorporating TMB in the structure-directing surfactant CTAB.[18,19] To have a better understanding of the role of TMB molecules on the size of the mesopores in the mesostructured MOFs, the effects of the TMB/CTAB molar ratio on the porosity properties of the MOFs were investigated, and the relevant results are summarized in Table 1.

Figure 2 shows representative N_2 adsorption–desorption isotherms and distributions of pore diameters for the mesostructured $[Cu_3(btc)_2(H_2O)_3]$ MOFs synthesized at a CTAB/Cu^{2+} molar ratio of 0.30 and at TMB/CTAB molar ratios of

Table 1: Synthesis conditions and porosity properties of the hierarchically micro- and mesoporous MOFs.

Sample	Molar ratio[a] $Cu^{2+}/H_3btc/CTAB/TMB$	S_{BET} [$m^2 g^{-1}$][b]	S_{micro} [$m^2 g^{-1}$][c]	S_{meso}/S_{micro}[c]	V_t [$cm^3 g^{-1}$][d]	V_{meso} [$cm^3 g^{-1}$][e]	V_{meso}/V_{micro}[e]	Mesopore diameter [nm][f]
1A	1:0.556:0.15:–	1225	1028	0.24	0.609	0.116	0.24	3.8
1B	1:0.556:0.30:–	1124	905	0.32	0.597	0.153	0.34	3.9
1C	1:0.556:0.60:–	905	721	0.34	0.560	0.170	0.44	5.6
2A	1:0.956:0.30:0.15	579	481	0.26	0.505	0.297	1.43	31.0
2B	1:0.956:0.30:0.30	533	420	0.36	0.517	0.321	1.64	23.0
2C	1:0.956:0.30:0.60	1124	936	0.25	0.575	0.111	0.24	4.9
3	1:0.956:0.60:0.30	738	596	0.31	0.514	0.226	0.78	14.9

[a] All samples were synthesized at a $Cu(NO_3)_2/H_2O/EtOH$ molar ratio of 1:185:60. [b] S_{BET} is the BET specific surface area. [c] S_{micro} is the *t*-plot specific micropore surface area calculated from the N_2 adsorption–desorption isotherm. S_{meso} is the specific mesopore surface area estimated by subtracting S_{micro} from S_{BET}. [d] V_t is the total specific pore volume determined by using the adsorption branch of the N_2 isotherm at $P/P_0 = 0.99$. [e] V_{meso} is the specific mesopore volume obtained from the BJH cumulative specific adsorption volume of pores of 1.70 to 300.00 nm in diameter. V_{micro} is the specific micropore volume calculated by subtracting V_{meso} from V_t. [f] The mesopore diameter is determined from the local maximum of the BJH distribution of pore diameters obtained in the adsorption branch of the N_2 isotherm.

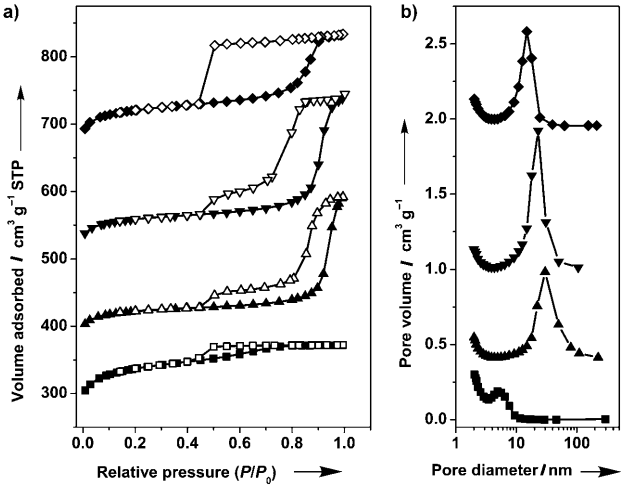

Figure 2. Pore-structure analysis of the hierarchically micro- and mesoporous MOFs **2A** (△), **2B** (▽), **2C** (□), and **3** (◇). a) N_2 adsorption–desorption isotherms; the isotherms for **2A**, **2B**, and **3** are vertically offset by 250, 400, and 500 $cm^3 g^{-1}$, respectively. b) Distributions of pore diameters obtained using the BJH method; the distributions for **2A**, **2B**, and **3** are vertically offset by 0.4, 1.0, and 2.0 $cm^3 g^{-1}$, respectively.

0.50 (**2A**), 1.0 (**2B**), and 2.0 (**2C**), as well as at a $CTAB/Cu^{2+}$ molar ratio of 0.60 and at a TMB/CTAB molar ratio of 0.50 (**3**). Remarkably, the mesopore diameter of the mesostructured MOF increases to 31.0 nm for **2A** with the addition of TMB to the reaction mixture at a TMB/CTAB molar ratio of 0.50 when the $CTAB/Cu^{2+}$ molar ratio is fixed at 0.30 (Figure 2b and Table 1). This result suggests that an expansion of the mesopore size of the framework can be achieved through the incorporation of TMB in the hydrophobic interior region of the micelles. However, a further increase of the TMB/CTAB molar ratio from 0.50 to 1.0 results in a decrease of the mesopore diameter to 23.0 nm for **2B** (Figure 2b and Table 1). Unexpectedly, the mesopore diameter of the mesostructured MOF decreases further to 4.9 nm for **2C** when the TMB/CTAB molar ratio is raised from 1.0 to 2.0 (Figure 2b and Table 1). These results are quite different from those obtained for inorganic mesoporous materials (for example, mesoporous silicas), for which the mesopore size is found to increase with an increase in the TMB/CTAB molar ratio,[18] indicating a difference between the assembly mechanisms of the mesostructured MOFs and inorganic mesoporous materials. In the case of the latter, inorganic compounds are commonly used as precursors. In the present work, however, the organic precursor (H_3btc) chosen as a ligand may significantly affect the structure-directing assembly of the mesostructured MOFs. Furthermore, the specific surface area, the S_{meso}/S_{micro} ratio, and the V_{meso}/V_{micro} ratio are tunable for the mesostructured MOFs by varying the molar ratio of the auxiliary structure-directing agent to the surfactant. As can be seen from Table 1, the BET surface area of the MOFs decreases remarkably from 1124 to 579 $m^2 g^{-1}$ with increasing TMB/CTAB molar ratio from 0 to 0.50. Accordingly, the V_{meso}/V_{micro} ratio increases significantly from 0.34 to 1.43 (Table 1). With an increase in the TMB/CTAB molar ratio from 0.50 to 1.0 at a fixed $CTAB/Cu^{2+}$ molar ratio of 0.30, the BET surface area of the sample decreases from 579 to 533 $m^2 g^{-1}$, while the S_{meso}/S_{micro} and V_{meso}/V_{micro} ratios increase from 0.26 to 0.36 and from 1.43 to 1.64, respectively (Table 1).

Although the results obtained from the N_2 adsorption–desorption isotherms and pore-size-distribution analyses for these mesostructured MOFs suggest that the mesopore diameters of these materials differ greatly from 3.8 to 31.0 nm, the small-angle X-ray diffraction (SAXD) patterns of the MOFs are indistinguishable (Figure S2). The SAXD patterns of all the MOFs exhibit a single low-angle diffraction peak at a $2\theta = 1.3°$, suggesting a disordered mesostructure without long-range order in the arrangement of the mesopores. The correlation peak indicates the average pore-to-pore separation in the disordered wormhole framework.[20] Wide-angle X-ray diffraction (WAXD) patterns of the as-synthesized samples (Figure S2) show the characteristic pattern of microporous $[Cu_3(btc)_2(H_2O)_3]$.[16] The weak and broad diffraction peaks indicate that the samples are composed of small crystals with a crystalline size on the nanoscale. The sizes of the crystallites in the solids estimated by applying the Scherrer formula on the 222 diffraction peak are approximately 17 to 22 nm. All these results suggest that the mesostructured MOFs consist of nanocrystalline domains of microporous $[Cu_3(btc)_2(H_2O)_3]$. This result is also con-

firmed by transmission electron microscopy (TEM) and selected-area electron diffraction (SAED; Figure S3).

Figure 3 shows several representative TEM images of the mesostructured MOFs. Note that it was quite difficult to obtain high-quality TEM images for these materials, not only because of the small mesopore diameters and pore volumes (especially for **1A–C** and **2C**), but also because the samples are highly sensitive to the electron beam. Furthermore, although mesoporous silicas and other mesostructured

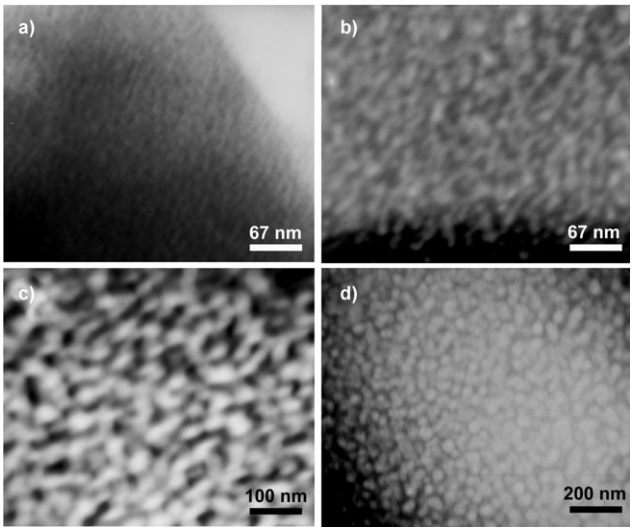

Figure 3. TEM images of the mesostructured MOFs: a) **1C**, b) **3**, c) **2B**, and d) **2A**.

metal oxides obtained with CTAB as a structure-directing agent have well-ordered mesoporous structures, TEM images of the MOFs synthesized in the present work demonstrate that the MOFs have disordered wormhole mesopore structures (Figure 3), which is consistent with the SAXD results. The accessible mesopores are connected randomly, and there is no discernible long-range mesopore ordering. The average pore diameters measured from the TEM images agree well with those derived from the N_2 adsorption–desorption isotherms.

An intraparticle porous topology is commonly regarded as a characteristic of disordered MCM-41-like hexagonal silicas and is generated through the template effect of the surfactant.[21] Although it is not currently clear whether a liquid-crystal phase is formed under the solvothermal conditions of the synthesis, surfactant micelles are believed to be responsible for the structure-directing assembly of the mesostructured MOFs in the present work. Firstly, the deprotonated organic ligand btc^{3-} may enter the solvent region to balance the cationic charge of the micelle surface. Electrostatic interactions between micelles of the cationic surfactant and the negatively charged btc^{3-} ions lead to positioning of the framework-building blocks. Secondly, nucleation and crystal-growth processes lead to nanoparticles of the microporous MOF, which are self-assembled from the framework-building blocks (that is, Cu^{2+} ions and the btc^{3-} ligand) in the continuous solvent region between micelles. After removal of the surfactant molecules from the solids, the hierarchically micro- and mesoporous MOFs are obtained.

In summary, the present work demonstrates a general methodology for the preparation of hierarchically micro- and mesoporous MOFs through an easy one-step templating process. This supramolecular template strategy enables us to rationally design and synthesize hierarchically porous MOFs with controllable porosity. An appropriate choice of supramolecular templates (for example, surfactants, block copolymers, and swelling agents) and a variation of the molar ratios of surfactant to framework-building blocks and of surfactant to swelling agent could be used to systematically control the porosity of such MOFs. Particularly, the size and shape of the micropores in such MOFs, as well as the functionality of the frameworks could also be easily tuned by choosing different framework-building blocks (that is, metal ions and organic ligands; see seminal works by Robson et al.[1a,22] and systematic studies by Yaghi et al.,[2,23] which have established the feasibility of the design of microporous MOFs with precisely controlled pore sizes and chemical functionalities). The hierarchically micro- and mesoporous MOFs with controllable porosity prepared herein have a good potential for application in bioengineering, sensing, heterogeneous catalysis, selective separation, and controlled release, because the presence of micro- and mesopores provides multiple benefits arising from each of the pore-size regimes.

Received: July 25, 2008
Published online: October 29, 2008

Keywords: mesoporous materials · metal–organic frameworks · microporous materials · organic–inorganic hybrid composites · zeolite analogues

[1] a) S. R. Batten, R. Robson, *Angew. Chem.* **1998**, *110*, 1558; *Angew. Chem. Int. Ed.* **1998**, *37*, 1460; b) C. N. R. Rao, S. Natarajan, R. Vaidhyanathan, *Angew. Chem.* **2004**, *116*, 1490; *Angew. Chem. Int. Ed.* **2004**, *43*, 1466; c) S. Kitagawa, R. Kitaura, S. Noro, *Angew. Chem.* **2004**, *116*, 2388; *Angew. Chem. Int. Ed.* **2004**, *43*, 2334.

[2] a) N. W. Ockwig, O. Delgado-Friedrichs, M. O'Keeffe, O. M. Yaghi, *Acc. Chem. Res.* **2005**, *38*, 176; b) M. Eddaoudi, D. B. Moler, H. L. Li, B. L. Chen, T. M. Reineke, M. O'Keeffe, O. M. Yaghi, *Acc. Chem. Res.* **2001**, *34*, 319; c) O. M. Yaghi, H. L. Li, C. Davis, D. Richardson, T. L. Groy, *Acc. Chem. Res.* **1998**, *31*, 474.

[3] U. Mueller, M. Schubert, F. Teich, H. Puetter, K. Schierle-Arndt, J. Pastre, *J. Mater. Chem.* **2006**, *16*, 626.

[4] a) J. L. C. Rowsell, O. M. Yaghi, *Angew. Chem.* **2005**, *117*, 4748; *Angew. Chem. Int. Ed.* **2005**, *44*, 4670; b) S. Q. Ma, H. C. Zhou, *J. Am. Chem. Soc.* **2006**, *128*, 11734.

[5] a) L. Pan, D. H. Olson, L. R. Ciemnolonski, R. Heddy, J. Li, *Angew. Chem.* **2006**, *118*, 632; *Angew. Chem. Int. Ed.* **2006**, *45*, 616; b) S. H. Jhung, J.-H. Lee, J. W. Yoon, C. Serre, G. Férey, J.-S. Chang, *Adv. Mater.* **2007**, *19*, 121.

[6] a) J. S. Seo, D. Whang, H. Lee, S. I. Jun, J. Oh, Y. J. Jeon, K. Kim, *Nature* **2000**, *404*, 982; b) L.-G. Qiu, A.-J. Xie, L.-D. Zhang, *Adv. Mater.* **2005**, *17*, 689; c) C.-D. Wu, W. Lin, *Angew. Chem.* **2007**, *119*, 1093; *Angew. Chem. Int. Ed.* **2007**, *46*, 1075.

[7] a) K. L. Wong, G. L. Law, Y. Y. Yang, W. T. Wong, *Adv. Mater.* **2006**, *18*, 1051; b) Y. Bai, G. J. He, Y. G. Zhao, C. Y. Duan, D. B. Dang, Q. J. Meng, *Chem. Commun.* **2006**, 1530; c) L.-G. Qiu, Z.-

Q. Li, Y. Wu, W. Wang, T. Xu, X. Jiang, *Chem. Commun.* **2008**, 3642.
[8] a) G. J. Halder, C. J. Kepert, B. Moubaraki, K. S. Murray, J. D. Cashion, *Science* **2002**, *298*, 1762; b) D. Maspoch, D. Ruiz-Molina, J. Veciana, *J. Mater. Chem.* **2004**, *14*, 2713; c) V. Niel, A. L. Thompson, M. C. Munoz, A. Galet, A. S. E. Goeta, J. A. Real, *Angew. Chem.* **2003**, *115*, 3890; *Angew. Chem. Int. Ed.* **2003**, *42*, 3760.
[9] X.-S. Wang, S. Ma, D. Sun, S. Parkin, H.-C. Zhou, *J. Am. Chem. Soc.* **2006**, *128*, 16474.
[10] G. Férey, C. Mellot-Draznieks, C. Serre, F. Millange, J. Dutour, S. Surblé, I. Margiolaki, *Science* **2005**, *309*, 2040.
[11] G. Férey, C. Serre, C. Mellot-Draznieks, F. Millange, S. Surblé, J. Dutour, I. Margiolaki, *Angew. Chem.* **2004**, *116*, 6456; *Angew. Chem. Int. Ed.* **2004**, *43*, 6296.
[12] Y. K. Park, et al., *Angew. Chem.* **2007**, *119*, 8378; *Angew. Chem. Int. Ed.* **2007**, *46*, 8230, see the Supporting Information.
[13] Q.-R. Fang, G.-S. Zhu, Z. Jin, Y.-Y. Ji, J.-W. Ye, M. Xue, H. Yang, Y. Wang, S.-L. Qiu, *Angew. Chem.* **2007**, *119*, 6758; *Angew. Chem. Int. Ed.* **2007**, *46*, 6638.
[14] a) M. E. Davis, *Nature* **2002**, *417*, 813; b) S. Hartmann, D. Brandhuber, N. Hüsing, *Acc. Chem. Res.* **2007**, *40*, 885.
[15] P. Yang, D. Zhao, D. I. Margolese, B. F. Chmelka, G. D. Stucky, *Nature* **1998**, *396*, 152.
[16] S. S.-Y. Cui, S. M.-F. Lo, J. P. H. Charmant, A. G. Orpen, I. D. Williams, *Science* **1999**, *283*, 1148.
[17] S. J. Gregg, K. S. W. Sing, *Adsorption, Surface Area and Porosity*, Academic Press, London, **1997**, pp. 111 – 194.
[18] J. S. Beck et al., *J. Am. Chem. Soc.* **1992**, *114*, 10834, see the Supporting Information.
[19] C. T. Kresge, M. E. Leonowicz, W. J. Roth, J. C. Vartuli, J. S. Beck, *Nature* **1992**, *359*, 710.
[20] T. R. Pauly, Y. Liu, T. J. Pinnavaia, S. J. L. Billinge, T. P. Rieker, *J. Am. Chem. Soc.* **1999**, *121*, 8835.
[21] J. El Haskouri, D. O. de Zárate, C. Guillem, A. Beltrán-Porter, M. Caldés, M. D. Marcos, D. Beltrán-Porter, J. Latorre, P. Amorós, *Chem. Mater.* **2002**, *14*, 4502.
[22] B. F. Hoskins, R. Robson, *J. Am. Chem. Soc.* **1990**, *112*, 1546.
[23] M. Eddaoudi, J. Kim, N. Rosi, D. Vodak, J. Wachter, M. O'Keeffe, O. M. Yaghi, *Science* **2002**, *295*, 469.

